

Properties of the η_q leading-twist distribution amplitude and its effects to the $B/D^+ \rightarrow \eta^{(\prime)} \ell^+ \nu_\ell$ decays

Dan-Dan Hu,^{1,*} Xing-Gang Wu,^{1,†} Hai-Bing Fu,^{2,‡} Tao Zhong,^{2,§} Zai-Hui Wu,^{2,¶} and Long Zeng^{1,**}

¹*Department of Physics, Chongqing Key Laboratory for Strongly Coupled Physics, Chongqing University, Chongqing 401331, P.R. China*

²*Department of Physics, Guizhou Minzu University, Guiyang 550025, P.R. China*

(Dated: July 11, 2023)

The $\eta^{(\prime)}$ -mesons in the quark-flavor basis are mixtures of two mesonic states $|\eta_q\rangle = (\bar{u}u + \bar{d}d)/\sqrt{2}$ and $|\eta_s\rangle = |\bar{s}s\rangle$. In the previous work, we have made a detailed study on the η_s leading-twist distribution amplitude. As a sequential work, in the present paper, we fix the η_q leading-twist distribution amplitude by using the light-cone harmonic oscillator model for its wave function and by using the QCD sum rules within the QCD background field to calculate its moments. The input parameters of η_q leading-twist distribution amplitude $\phi_{2;\eta_q}$ at an initial scale $\mu_0 \sim 1$ GeV are then fixed by using those moments. The sum rules for the 0_{th}-order moment can also be used to fix the magnitude of η_q decay constant, which gives $f_{\eta_q} = 0.141 \pm 0.005$ GeV. As an application of the present derived $\phi_{2;\eta_q}$, we calculate the transition form factors $B(D)^+ \rightarrow \eta^{(\prime)}$ by using the QCD light-cone sum rules up to twist-4 accuracy and by including the next-to-leading order QCD corrections to the twist-2 part, and then fix the related CKM matrix element and the decay width for the semi-leptonic decays $B(D)^+ \rightarrow \eta^{(\prime)} \ell^+ \nu_\ell$.

PACS numbers: 13.25.Hw, 11.55.Hx, 12.38.Aw, 14.40.Be

I. INTRODUCTION

The mixing of η and η' mesons is essential to disentangle the standard model (SM) hadronic uncertainties with the new physics beyond the SM. It involves the dynamics and structure of the pseudoscalar mesons that has two mixing modes $\eta - \eta'$ and $\eta - \eta' - G$, both of which have important theoretical significance. These mixings are caused by the QCD anomalies and are related to the breaking of chiral symmetry. However, since the matrix element of the exception operator is mainly non-perturbative, it still has not been calculated reliably. One may turn to phenomenological studies to obtain useful information on the non-perturbative QCD theory [1–3]. At present, the $\eta - \eta' - G$ mixing mode has been studied in detail in Refs [4–10]. As for the $\eta - \eta'$ mixing model, one can investigate it by using two distinct schemes, namely the singlet-octet (SO) scheme and the quark-flavor (QF) scheme. These two schemes reflect different understandings of the essential physics and they are related with a proper rotation of an ideal mixing angle [3]. Practically, a dramatic simplification can be achieved by adopting the QF scheme [11–13], especially, the decay constants in the quark-flavor basis simply follow the same pattern of the state mixing due to the OZI-rule. In QF scheme, the physical meson states $|\eta\rangle$ and $|\eta'\rangle$ are related to the

QF basis $|\eta_q\rangle = (\bar{u}u + \bar{d}d)/\sqrt{2}$ and $|\eta_s\rangle = |\bar{s}s\rangle$ by an orthogonal transformation [13],

$$\begin{pmatrix} |\eta\rangle \\ |\eta'\rangle \end{pmatrix} = \begin{pmatrix} \cos\phi & -\sin\phi \\ \sin\phi & \cos\phi \end{pmatrix} \begin{pmatrix} |\eta_q\rangle \\ |\eta_s\rangle \end{pmatrix}, \quad (1)$$

where ϕ is the mixing angle. In the present paper, we shall adopt the QF scheme to do our analysis and to achieve a better understanding of the mixing mechanism between η and η' .

The $B(D) \rightarrow \eta^{(\prime)}$ transitions are important, since they involve $b \rightarrow u$ and $c \rightarrow d$ transitions and are sensitive to the CKM matrix elements $|V_{ub}|$ and $|V_{cd}|$. A more accurate determination of $|V_{ub}|$ and $|V_{cd}|$ would improve the stringency of unitarity constraints on the CKM matrix elements and provides an improved test of standard model (SM). Many measurements on $|V_{ub}|$ and $|V_{cd}|$ have been done according to various decay channels of $B(D)$ -mesons [14–23]. Compared with the non-leptonic $B(D)$ -meson decays, the semi-leptonic decays $D^+ \rightarrow \eta^{(\prime)} \ell^+ \nu_\ell$ [24–27] and $B^+ \rightarrow \eta^{(\prime)} \ell^+ \nu_\ell$ [14, 28–31] are much simpler with less non-perturbative effects and can serve as helpful platforms for exploring the differences among various mechanisms.

As key components of the $B(D) \rightarrow \eta^{(\prime)}$ semileptonic decays, the $B(D) \rightarrow \eta^{(\prime)}$ transition form factors (TFFs) need to be precisely calculated, whose main contribution comes from the $|\eta_q\rangle$ -component (the $|\eta_s\rangle$ -component gives negligible contribution here, but will have sizable contribution for B_s (D_s) decays [22]). By further assuming $SU_F(3)$ symmetry, the TFFs $f_+^{B(D) \rightarrow \eta^{(\prime)}}$ satisfy the following relation [22, 32]

$$f_+^{B(D) \rightarrow \eta} = \cos\phi f_+^{B(D) \rightarrow \eta_q}, \quad (2)$$

$$f_+^{B(D) \rightarrow \eta'} = \sin\phi f_+^{B(D) \rightarrow \eta_q}. \quad (3)$$

*Electronic address: hudd@stu.cqu.edu.cn

†Electronic address: wuxg@cqu.edu.cn

‡Electronic address: fuhb@cqu.edu.cn

§Electronic address: zhongtao1219@sina.com

¶Electronic address: wuzaihui@hotmail.com

**Electronic address: zlong@cqu.edu.cn

The TFFs of the heavy-to-light transitions at large and intermediate momentum transfers are among the most important applications of the light-cone sum rules (LCSR) approach. Using the LCSR approach, a two-point correlation function will be introduced and expanded near the light cone $x^2 \rightarrow 0$, whose transition matrix elements are then parameterized as the light meson's light-cone distribution amplitudes (LCDAs) of increasing twists [33–36]. It is thus important to know the properties of the LCDAs.

In the present paper, we will adopt the light cone harmonic oscillator (LCHO) model for the η_q leading-twist LCDA $\phi_{2;\eta_q}$. The LCHO model is based on the Brodsky-Huang-Lepage (BHL) prescription [37, 38]¹ for the light-cone wavefunction (LCWF), which is composed of the spin-space LCWF and the spatial one. The LCDA can be obtained by integrating over the transverse momentum from the LCWF. The parameters of $\phi_{2;\eta_q}$ at an initial scale will be fixed by using the derived moments of the LCDA, which will then be run to any scale region via proper evolution equation. Its moments will be calculated by using the QCD sum rules within the framework of the background field theory (BFTSR) [39, 40]. The QCD sum rules method suggests to use the non-vanishing vacuum condensates to represent the non-perturbative effects [41]. The QCD background field approach provides a description for those vacuum condensates from the viewpoint of field theory [42–45]. It assumes that the quark and gluon fields are composed of the background fields and the quantum fluctuations around them. And the vacuum expectation values of those background fields describe the non-perturbative effects, while the quantum fluctuations represent the calculable perturbative effects. As a combination, the BFTSR approach provides a clean physical picture for separating the perturbative and non-perturbative properties of the QCD theory and provides a systematic way to derive the QCD sum rules for hadron phenomenology. At the present, the BFTSR approach has been successfully applied for dealing with the LCDAs of various mesons, some recent examples can be found in Refs.[46–50].

The remaining parts of the paper are organized as follows. In Sec. II, we give the calculation technology for the moments of the η_q leading-twist LCDA $\phi_{2;\eta_q}$ by using the BFTSR approach, give a brief introduction of the LCHO model of $\phi_{2;\eta_q}$, and then give the LCSR to the semi-leptonic decay $B(D)^+ \rightarrow \eta_q \ell^+ \nu_\ell$. In Sec. III, we first determine the parameters of $\phi_{2;\eta_q}$. Finally, the TFF, the decay width and the CKM matrix element of the semi-leptonic decay $B(D)^+ \rightarrow \eta^{(\prime)} \ell^+ \nu_\ell$ will be discussed. We will also compare our results with the experimental data

and other theoretical predictions. Sec. IV is reserved for a summary.

II. CALCULATION TECHNOLOGY

A. Determination of the moments $\langle \xi_{2;\eta_q}^n \rangle$ of the η_q twist-2 LCDA using the BFTSR

To determine the distribution amplitude, one can calculate firstly the moment of the distribution amplitude. The $\eta^{(\prime)}$ meson twist-2 LCDA is defined as [9, 10]

$$\begin{aligned} & \langle 0 | \bar{\Psi}(z) \mathcal{C}_i [z, -z] \not{z} \gamma_5 \Psi(-z) | \eta^{(\prime)}(q) \rangle \\ &= i(z \cdot q) f_\eta \int_0^1 dx e^{i(2x-1)(z \cdot q)} \phi_{2;\eta^{(\prime)}}(x, \mu) \end{aligned} \quad (4)$$

where $\Psi = (u, d, s)$ represents the triplet of the light-quark fields in the flavour space, $[z, -z]$ is the path-ordered gauge connection which ensures the gauge invariance of the operator, and $\phi_{2;\eta^{(\prime)}}(x, \mu)$ is the twist-2 LCDA of the η meson with respect to the current whose flavour content is given by $\mathcal{C}_i (i = q, s)$. And we have $\mathcal{C}_q = (\sqrt{2}\mathcal{C}_1 + \mathcal{C}_8)/\sqrt{3}$ and $\mathcal{C}_s = (\mathcal{C}_1 - \sqrt{2}\mathcal{C}_8)/\sqrt{3}$ with $\mathcal{C}_1 = \mathbf{1}/\sqrt{3}$ and $\mathcal{C}_8 = \lambda_8/\sqrt{2}$ which are derived in singlet-octet scheme [9], where λ_8 is the standard Gell-Mann matrix and $\mathbf{1}$ is 3×3 unit matrix. The $\eta^{(\prime)}$ -meson twist-2 two-quark LCDAs are symmetric in the QF basis [10].

In line with the implementation of the QF scheme for the η_q twist-2 LCDA, an approximation is implicitly adopted, i.e. $\langle 0 | \bar{\Psi}(z) \mathcal{C}_q [z, -z] \not{z} \gamma_5 \Psi(-z) | \eta_q(q) \rangle = \langle 0 | \bar{u}(z) [z, -z] \not{z} \gamma_5 d(-z) | \pi^-(q) \rangle$ [9]. That is, the definition of the η_q meson is the same as that of the π^0 meson. According to the definition, we have

$$\begin{aligned} & \frac{\mathcal{C}_q}{\sqrt{2}} \langle 0 | [\bar{u}(0) \not{z} \gamma_5 (iz \cdot \vec{D})^n u(0) + \bar{d}(0) \not{z} \gamma_5 (iz \cdot \vec{D})^n d(0)] | \eta_q(q) \rangle \\ &= i(z \cdot q)^{n+1} f_{\eta_q} \langle \xi_{2;\eta_q}^n \rangle |_\mu, \end{aligned} \quad (5)$$

where μ is an initial scale. The η_q twist-2 LCDA $\phi_{2;\eta_q}$ and the n_{th} -order moment satisfy the equation,

$$\langle \xi_{2;\eta_q}^n \rangle |_\mu = \int_0^1 dx (2x-1)^n \phi_{2;\eta_q}(x, \mu). \quad (6)$$

Once the insert current is determined, the first step is to construct the correlation function (correlator)

$$\begin{aligned} \Pi_{2;\eta_q}^{(n,0)} &= i \int d^4x e^{iq \cdot x} \langle 0 | T \{ J_n(x), J_0^\dagger(0) \} | 0 \rangle \\ &= (z \cdot q)^{n+2} \Pi_{2;\eta_q}^{(n,0)}(q^2), \end{aligned} \quad (7)$$

For the QF basis, one may have two independent axial vector currents $J_{\mu 5}^q (q = u, d)$ and $J_{\mu 5}^s$. We have discussed $J_{\mu 5}^s$ in our previous work [51] for the case of η_s , and in

¹ The BHL-prescription is obtained in this way by connecting the equal-time wavefunction in the rest frame and the wavefunction in the infinite momentum frame, which indicates that the LCWF should be a function of the meson's off-shell energy.

this paper, we will focus on $J_{\mu 5}^q$ ($q = u, d$) for the present case of η_q . Then the required currents in the correlator can be defined as $J_n(x) = \frac{C_q}{\sqrt{2}}[\bar{u}(x)\not{x}\gamma_5(iz \cdot \overleftrightarrow{D})^n u(x) + \bar{d}(x)\not{x}\gamma_5(iz \cdot \overleftrightarrow{D})^n d(x)] = \bar{u}(x)\not{x}\gamma_5(iz \cdot \overleftrightarrow{D})^n d(x)$ [9], where $z^2 = 0$. It is found that even moments are non-zero and the odd moments of the LCDA are zero because of the G -parity, then only the $n = (0, 2, 4, \dots)$ will be considered.

For the second step, the correlator can be calculated by inserting a complete set of intermediate hadronic states in physical region. Based on the quark-hadron duality, the hadron expression can be obtained

$$\text{Im}I_{2;\eta_q, \text{Had}}^{(n,0)}(q^2) = \pi\delta(q^2 - \tilde{m}_{\eta_q}^2)f_{\eta_q}^2 \langle \xi_{2;\eta_q}^n \rangle |_{\mu} \langle \xi_{2;\eta_q}^0 \rangle |_{\mu} + \pi \frac{3}{4\pi^2(n+1)(n+3)} \theta(q^2 - s_{\eta_q}) \quad (8)$$

$$\begin{aligned} \langle \xi_{2;\eta_q}^n \rangle |_{\mu} \langle \xi_{2;\eta_q}^0 \rangle |_{\mu} = & \frac{M^2}{f_{\eta_q}^2} e^{\tilde{m}_{\eta_q}^2/M^2} \left\{ \frac{3}{4\pi^2(n+1)(n+3)} (1 - e^{-s_{\eta_q}/M^2}) + \frac{(m_u + m_d)\langle \bar{q}q \rangle}{M^4} + \frac{\langle \alpha_s G^2 \rangle}{12\pi M^4} \frac{1 + n\theta(n-2)}{n+1} \right. \\ & - \frac{(m_u + m_d)\langle g_s \bar{q}\sigma T G q \rangle}{M^6} \frac{8n+1}{18} + \frac{\langle g_s \bar{q}q \rangle^2}{M^6} \frac{4(2n+1)}{18} - \frac{\langle g_s^3 f G^3 \rangle}{M^6} \frac{n\theta(n-2)}{48\pi^2} + \frac{\langle g_s^2 \bar{q}q \rangle^2}{M^6} \frac{2 + \kappa^2}{486\pi^2} \\ & \times \left\{ -2(51n+25) \left(-\ln \frac{M^2}{\mu^2} \right) + 3(17n+35) + \theta(n-2) \left[2n \left(-\ln \frac{M^2}{\mu^2} \right) + \frac{49n^2 + 100n + 56}{n} \right. \right. \\ & \left. \left. - 25(2n+1) \left[\psi \left(\frac{n+1}{2} \right) - \psi \left(\frac{n}{2} \right) + \ln 4 \right] \right] \right\} \quad (9) \end{aligned}$$

It has been shown that due to the anomalous dimension of the n_{th} -order moment grows with increment of n , the contribution of the much higher moments at the large momentum transfer shall be highly suppressed [53]. Thus one may only need to calculate the first few ones. Specifically, the sum rule of the 0_{th}-order moment is

$$\begin{aligned} (\langle \xi_{2;\eta_q}^0 \rangle |_{\mu})^2 = & \frac{M^2}{f_{\eta_q}^2} e^{\tilde{m}_{\eta_q}^2/M^2} \left\{ \frac{1}{4\pi^2} \left(1 - e^{-s_{\eta_q}/M^2} \right) \right. \\ & + \frac{(m_u + m_d)\langle \bar{q}q \rangle}{M^4} - \frac{(m_u + m_d)\langle g_s \bar{q}\sigma T G q \rangle}{18M^6} \\ & + \frac{\langle \alpha_s G^2 \rangle}{12\pi M^4} + \frac{4\langle g_s \bar{q}q \rangle^2}{18M^6} + \frac{\langle g_s^2 \bar{q}q \rangle^2}{M^6} \frac{2 + \kappa^2}{486\pi^2} \\ & \left. \times \left[-50 \left(-\ln \frac{M^2}{\mu^2} \right) + 105 \right] \right\}. \quad (10) \end{aligned}$$

Due to the particularity of quark composition of η -meson, we take the η_q mass appeared in Eqs. (9) and (10) as its effective mass 370 MeV [52]. We use the equation $\langle \xi_{2;\eta_q}^n \rangle |_{\mu} = \langle \xi_{2;\eta_q}^n \rangle |_{\mu} \langle \xi_{2;\eta_q}^0 \rangle |_{\mu} / \sqrt{(\langle \xi_{2;\eta_q}^0 \rangle |_{\mu})^2}$ to calculate the moment [54]. The decay constant is an important input for the $B(D) \rightarrow \eta^{(\prime)}$ TFFs, which has been calculated under different methods such as the LCSR [55], the QCD sum rules (QCD SR) [56, 57], the light-front quark model

Because of the SU(3) flavour symmetric, here \tilde{m}_{η_q} is the η_q effective mass [52], f_{η_q} is the decay constant of η_q and s_{η_q} stands for the continuum threshold.

For the third step, one can apply the operator product expansion (OPE) to deal with the correlator in the deep Euclidean region. It is calculable and can be carried out within the framework of BFTSR. Detailed calculation processes can be found in Ref. [51]. The fourth step is to match the hadron expression corresponding to the correlator and the results obtained by OPE using the dispersion relation. After applying the Borel transformation for both sides so as to suppress the unwanted contributions from the even higher-order dimensional condensates, the sum rules for the moments of the η_q leading-twist LCDA $\phi_{2;\eta_q}(x, \mu)$ can be finally obtained, which takes the following form

(LFQM) [58–61], the lattice QCD (LQCD) [62–65], the Bethe-Salpeter (BS) model [66–68], the relativistic quark model (RQM) [69–71], the non-relativistic quark model (NRQM) [72], and etc.. As for the decay constant f_{η_q} , those studies shows that f_{η_q} is within a broader range [0.130, 0.168] GeV. At present, the sum rule of the η_q decay constant can be inversely obtained by using Eq.(10). The $\langle \xi_{2;\eta_q}^0 \rangle |_{\mu}$ should be normalized in a suitable Borel window, which will be treated as an important criteria for determining the η_q decay constant.

B. The LCHO model for η_q twist-2 LCDA

The meson's LCDA can be derived from its light-cone wave-function (LCWF) by integrating its transverse components. It is helpful to construct the η_q leading-twist LCWF and then get its LCDA [73, 74]. Practically, the η_q wave-function can be constructed by using the BHL prescription, and the LCHO model takes the form [54]:

$$\psi_{2;\eta_q}(x, \mathbf{k}_{\perp}) = \chi_{2;\eta_q}(x, \mathbf{k}_{\perp}) \psi_{2;\eta}^R(x, \mathbf{k}_{\perp}), \quad (11)$$

where \mathbf{k}_{\perp} is the η_q transverse momentum, $\chi_{2;\eta_q}(x, \mathbf{k}_{\perp})$ stands for the spin-space WF that comes from the

Wigner-Melosh rotation and the spatial WF $\psi_{2;\eta_q}^R(x, \mathbf{k}_\perp)$ comes from the approximate bound-state solution in the quark model for η_q , which the detailed expressions can be found in Ref [54]. Using the following relationship between the η_q twist-2 LCDA and LCWF,

$$\phi_{2;\eta_q}(x, \mu) = \frac{2\sqrt{6}}{f_{\eta_q}} \int_0^{|\mathbf{k}_\perp|^2 \leq \mu^2} \frac{d^2\mathbf{k}_\perp}{16\pi^3} \psi_{2;\eta_q}(x, \mathbf{k}_\perp), \quad (12)$$

and by integrating over the transverse momentum \mathbf{k}_\perp , one can get the twist-2 LCDA $\phi_{2;\eta_q}(x, \mu)$, which can be read off,

$$\begin{aligned} \phi_{2;\eta_q}(x, \mu) &= \frac{\sqrt{3}A_{2;\eta_q}m_q\beta_{2;\eta_q}}{2\sqrt{2}\pi^{3/2}f_{\eta_q}} \sqrt{x\bar{x}}\varphi_{2;\eta_q}(x) \\ &\times \left\{ \text{Erf} \left[\sqrt{\frac{m_q^2 + \mu^2}{8\beta_{2;\eta_q}^2 x\bar{x}}} \right] - \text{Erf} \left[\sqrt{\frac{m_q^2}{8\beta_{2;\eta_q}^2 x\bar{x}}} \right] \right\}. \end{aligned} \quad (13)$$

where $q = (u, d)$, m_q is the constituent quark mass. The main difference of the model parameters is the constituent quark mass, i.e. $m_u = m_d = 250$ MeV in the spin-averaged meson mass scheme [75], $m_u = m_d = 330$ GeV in the invariant meson mass scheme [76, 77] and $m_u = m_d = 300$ MeV for the simplest in Refs [78, 79]. In principle, the hadron function determines all properties of hadrons. From the relation between wavefunction and measurability, we can obtain some constraints on the general properties of hadronic function. We will constraint the parameters $A_{2;\eta_q}$ and $\beta_{2;\eta_q}$ according to the following two constraints.

Both the pseudoscalar and vector mesons one constraint on the wavefunction is from the leptonic decay processes. The WF normalization condition provided from the process $\eta_q \rightarrow \mu\nu$

$$\int_0^1 dx \int \frac{d^2\mathbf{k}_\perp}{16\pi^3} \psi_{2;\eta_q}(x, \mathbf{k}_\perp) = \frac{f_{\eta_q}}{2\sqrt{6}}. \quad (14)$$

The second constraint is the most natural one: the probability of finding the $q\bar{q}$ Fock state in a meson should be not larger than 1,

$$\begin{aligned} P_{\eta_q} &= \int_0^1 dx \int \frac{d^2\mathbf{k}_\perp}{16\pi^3} |\psi_{2;\eta_q}(x, \mathbf{k}_\perp)|^2 \\ &= \frac{A_{2;\eta_q}^2 m_q^2}{32\pi^2} [\varphi_{2;\eta_q}(x)]^2 \Gamma \left[0, \frac{m_q^2}{4\beta_{2;\eta_q}^2 x\bar{x}} \right]. \end{aligned} \quad (15)$$

Since pionic twist-2 wavefunction conforms to the probability $P_\pi \approx 0.3$ [74], we adopt $P_{\eta_q} \approx 0.3$ to carry out the following calculation. Equivalently, one can replace the constraint (15) by the quark transverse momentum $\langle \mathbf{k}_\perp^2 \rangle_{\eta_q}$, which is measurable and is defined as [74]

$$\langle \mathbf{k}_\perp^2 \rangle_{\eta_q} = \int_0^1 dx \int \frac{d^2\mathbf{k}_\perp}{16\pi^3} |\mathbf{k}_\perp^2| \psi_{2;\eta_q}^R(x, \mathbf{k}_\perp)^2 / P_{\eta_q}$$

$$= \int_0^1 dx \frac{4 \exp \left[-\frac{m_q^2}{4x\bar{x}\beta_{2;\eta_q}^2} \right] x\bar{x}\beta_{2;\eta_q}^2}{\Gamma \left[0, \frac{m_q^2}{4x\bar{x}\beta_{2;\eta_q}^2} \right]} - m_q^2 \quad (16)$$

where the incomplete gamma function $\Gamma[s, x] = \int_0^x t^{s-1} e^{-t} dt$.

The function $\varphi_{2;\eta_q}(x)$ determines the dominant longitudinal behavior of $\phi_{2;\eta_q}(x, \mu^2)$, which can be expanded as a Gegenbauer series as

$$\varphi_{2;\eta_q}(x) = \left[1 + \sum_n B_n \times C_n^{3/2}(2x-1) \right], \quad (17)$$

For self-consistency, it has been found that the parameters B_n are close to their corresponding Gegenbauer moment, i.e. $B_n \sim a_n$, especially for the first few ones [79–81]. The η_q meson Gegenbauer moments can be calculated by the following way

$$a_{2;\eta_q}^n(\mu) = \frac{\int_0^1 dx \phi_{2;\eta_q}(x, \mu) C_n^{3/2}(2x-1)}{\int_0^1 dx 6x(1-x) [C_n^{3/2}(2x-1)]^2} \quad (18)$$

The Gegenbauer moments $a_{2;\eta_q}^n(\mu)$ and the DA moments $\langle \xi_{2;\eta_q}^n \rangle |_\mu$ satisfy the following relations

$$\begin{aligned} \langle \xi_{2;\eta_q}^2 \rangle |_\mu &= \frac{1}{5} + \frac{12}{35} a_{2;\eta_q}^2(\mu) \\ \langle \xi_{2;\eta_q}^4 \rangle |_\mu &= \frac{3}{35} + \frac{8}{35} a_{2;\eta_q}^2(\mu) + \frac{8}{77} a_{2;\eta_q}^4(\mu) \\ &\dots \end{aligned} \quad (19)$$

By using the sum rules (9) of $\langle \xi_{2;\eta_q}^n \rangle |_\mu$, one can determine the values of $a_{2;\eta_q}^n(\mu)$, which then can be used to fix the values of B_n . In the following we will adopt the given two Gegenbauer moments $a_{2;\eta_q}^{2,4}$ to fix the parameters $B_{2,4}$.

C. The $B(D)^+ \rightarrow \eta_q \ell^+ \nu_\ell$ TFFs using the LCSR

The LCSR approach is an effective tool in determining the non-perturbative properties of hadronic states. Here and after, we use the symbol “ H ” to indicate the $B(D)$ -meson for convenience. Following the LCSR approach, one should first construct a correlator with the weak current and a current with the quantum numbers of the H meson that are sandwiched between the vacuum and η_q state. More explicitly, for $H \rightarrow \eta_q$, we need to calculate the correlator

$$\begin{aligned} \Pi_\mu(p, q) &= i \int d^4x e^{iqx} \langle \eta_q(p) | T \{ \bar{u}(x) \gamma_\mu Q(x), j_H(0) \} | 0 \rangle \\ &= \Pi[q^2, (p+q)^2] p_\mu + \tilde{\Pi}[q^2, (p+q)^2] q_\mu. \end{aligned} \quad (20)$$

where $j_H = (m_Q \bar{Q} i \gamma_5 d)$ with $Q = (b, c)$ -quark for (B, D) meson, respectively. The LCSR calculation for the

$B(D)^+ \rightarrow \eta_q$ TFFs is similar to the case of $B_s(D_s) \rightarrow \eta_s$, which has been done in Ref.[51]. In the following, we will give the main procedures for self-consistency, and the interesting reader may turn to Ref.[51] for more detail.

The dual property of the correlator (20) is used to connect the two different representations in different momentum transfer regions. In the time-like region, one can insert a complete set of the intermediate hadronic states in the correlator and obtain its hadronic representation by isolating out the pole term of the lowest meson state, i.e.

$$\begin{aligned} \Pi_\mu^{\text{had}}(p, q) &= \frac{\langle \eta_q(p) | \bar{u} \gamma_\mu Q | H(p+q) \rangle \langle H(p+q) | \bar{Q} i \gamma_5 q | 0 \rangle}{m_H^2 - (p+q)^2} \\ &+ \sum_{\mathcal{H}} \frac{\langle \eta_q(p) | \bar{u} \gamma_\mu Q | H^{\mathcal{H}}(p+q) \rangle \langle H^{\mathcal{H}}(p+q) | \bar{Q} i \gamma_5 q | 0 \rangle}{m_{H^{\mathcal{H}}}^2 - (p+q)^2} \\ &= \Pi^{\text{had}}[q^2, (p+q)^2] p_\mu + \tilde{\Pi}^{\text{had}}[q^2, (p+q)^2] q_\mu, \end{aligned} \quad (21)$$

where the superscript ‘‘had’’ and ‘‘ \mathcal{H} ’’ stand for the hadronic expression of the correlator and the continuum states of heavy meson, respectively. Here, the decay constant of $B(D)$ -meson is defined via the equation, $\langle H | \bar{Q} i \gamma_5 q | 0 \rangle = m_H^2 f_H / m_Q$, and by using the hadronic dispersion relations in the virtuality $(p+q)^2$ of the current in the $B(D)$ channel, we can relate the correlator to the $H \rightarrow \eta_q$ matrix element [9]

$$\begin{aligned} \langle \eta_q(p) | \bar{u} \gamma_\mu Q | H(p+q) \rangle &= 2p_\mu f_+^{H \rightarrow \eta_q}(q^2) \\ &+ q_\mu \left(f_+^{H \rightarrow \eta_q}(q^2) + f_-^{H \rightarrow \eta_q}(q^2) \right). \end{aligned} \quad (22)$$

Due to chiral suppression, only the first term contributes to the semileptonic decay of $H \rightarrow \eta_q$ with massless leptons in the final state. Then, the hadronic expression for the invariant amplitude can be written as

$$\begin{aligned} \Pi[q^2, (p+q)^2] &= \frac{2m_H^2 f_H f_+^{H \rightarrow \eta_q}(q^2)}{[m_H^2 - (p+q)^2]} p_\mu \\ &+ \int_{s_0}^{\infty} ds \frac{\rho^{\mathcal{H}}(q^2, s)}{s - (p+q)^2}, \end{aligned} \quad (23)$$

where s_0 is continuum threshold parameter, $\rho^{\mathcal{H}}$ is the hadronic spectral density.

In the space-like region, the correlator can be calculated by using the operator production expansion (OPE). The OPE near the light cone $x^2 \approx 0$ leads to a convolution of perturbatively calculable hard-scattering amplitudes and universal soft LCDAs. Since the contributions of the three-particle part is small [51], we only calculate the two-particle part here, and the corresponding matrix element is [82]

$$\begin{aligned} \langle \eta_q(p) | \bar{u}_\alpha^i(x) d_\beta^j(0) | 0 \rangle &= \frac{i \delta^{ij}}{12} f_{\eta_q} \int_0^1 du e^{iup \cdot x} \left\{ [\not{p} \gamma_5]_{\beta\alpha} \phi_{2;\eta_q}(u) \right. \\ &(u) - [\gamma_5]_{\beta\alpha} \mu_{\eta_q} \phi_{3;\eta_q}^p(u) + \frac{1}{6} [\sigma_{\nu\tau} \gamma_5]_{\beta\alpha} p_\nu x_\tau \mu_{\eta_q} \phi_{3;\eta_q}^\sigma(u) \\ &\left. + \frac{1}{16} [\not{p} \gamma_5]_{\beta\alpha} x^2 \phi_{4;\eta_q}(u) - \frac{i}{2} [\not{x} \gamma_5]_{\beta\alpha} \int_0^u \psi_{4;\eta_q}(v) dv \right\} \end{aligned} \quad (24)$$

The light-cone expansion for $q^2, (p+q)^2 \ll m_b^2$ (or m_c^2), the correlator Π^{OPE} can be written in the general form

$$\begin{aligned} \Pi^{\text{OPE}}[q^2, (p+q)^2] &= F_0(q^2, (p+q)^2) \\ &+ \frac{\alpha_s C_F}{4\pi} F_1(q^2, (p+q)^2). \end{aligned} \quad (25)$$

In the above equation, the first term is the leading-order (LO) for all the LCDAs' contributions, and the second term stands for the gluon radiative corrections to the dominant twist-2 parts.

After an analytic continuation of the light-cone expansion to physical momenta using a dispersion relations, one equates the above two representations by the assumption of quark-hadron duality. Then to get the final LCSR, we need to do the Borel transformation, which results in

$$\begin{aligned} f_+^{H \rightarrow \eta_q}(q^2) &= \frac{e^{m_H^2/M^2}}{2m_H^2 f_H} \left[F_0(q^2, M^2, s_0) \right. \\ &\left. + \frac{\alpha_s C_F}{4\pi} F_1(q^2, M^2, s_0) \right], \end{aligned} \quad (26)$$

where F_0 (F_1) represents the leading-order (LO) or next-to-leading order (NLO) contribution, respectively. Our final LCSR for the $H \rightarrow \eta_q$ TFF is

$$\begin{aligned} f_+^{H \rightarrow \eta_q}(q^2) &= \frac{m_Q^2 f_{\eta_q}}{2m_H^2 f_H} e^{m_H^2/M^2} \int_{u_0}^1 du e^{-s(u)/M^2} \left\{ \frac{\phi_{2;\eta_q}(u)}{u} + \frac{\mu_{\eta_q}}{m_Q} \left[\phi_{3;\eta_q}^p(u) + \frac{1}{6} \left(2 \frac{\phi_{3;\eta_q}^\sigma(u)}{u} - \frac{m_Q^2 + q^2 - u^2 m_\eta^2}{m_Q^2 - q^2 + u^2 m_\eta^2} \right) \right. \right. \\ &\times \left. \frac{d}{du} \phi_{3;\eta_q}^\sigma(u) + \frac{4um_\eta^2 m_Q^2}{(m_Q^2 - q^2 + u^2 m_\eta^2)^2} \phi_{3;\eta_q}^\sigma(u) \right] + \frac{1}{m_Q^2 - q^2 + u^2 m_\eta^2} \left[u \psi_{4;\eta_q}(u) + \left(1 - \frac{2u^2 m_\eta^2}{m_Q^2 - q^2 + u^2 m_\eta^2} \right) \right. \\ &\times \left. \int_0^u dv \psi_{4;\eta_q}(v) - \frac{m_Q^2}{4} \frac{u}{m_Q^2 - q^2 + u^2 m_\eta^2} \left(\frac{d^2}{du^2} - \frac{6um_\eta^2}{m_Q^2 - q^2 + u^2 m_\eta^2} \frac{d}{du} + \frac{12um_\eta^4}{(m_Q^2 - q^2 + u^2 m_\eta^2)^2} \right) \phi_{4;\eta_q}(u) \right] \\ &+ \frac{\alpha_s C_F e^{m_H^2/M^2}}{8\pi m_H^2 f_H} F_1(q^2, M^2, s_0), \end{aligned} \quad (27)$$

where $\bar{u} = (1 - u)$, $\mu_{\eta_q} = m_\eta^2/(m_u + m_d)$, $s(u) = (m_Q^2 - \bar{u}q^2 + u\bar{u}m_\eta^2)/u$ and $u_0 = (q^2 - s_0 + m_\eta^2 + \sqrt{(q^2 - s_0 + m_\eta^2)^2 - 4m_\eta^2(q^2 - m_Q^2)})/2m_\eta^2$. The invariant amplitude $F_1(q^2, M^2, s_0)$ has been given in Ref. [51], which can be written as a factorized form of the convolutions. As will be shown below, the high-twist terms will have quite small contributions to compare with the leading-twist terms, thus we will not discuss the uncertainties caused by the different choices of the high-twist LCDAs. For convenience, we take the η_q twist-3 LCDAs $\phi_{3;\eta_q}^p(u)$, $\phi_{3;\eta_q}^\sigma(u)$, and the twist-4 LCDAs $\psi_{4;\eta_q}(u)$, $\phi_{4;\eta_q}(u)$, together with their parameters from Ref. [10].

Using the resultant $B(D) \rightarrow \eta^{(\prime)}$ TFFs, one can extract the CKM matrix element $|V_{cd}|$ or $|V_{ub}|$ by comparing with the predictions with the experimental data, i.e. via the following equation [83]

$$\frac{\mathcal{B}(H \rightarrow \eta^{(\prime)} \ell \nu_\ell)}{\tau(H)} = \int_0^{q_{\max}^2} \frac{d\Gamma}{dq^2}(H \rightarrow \eta^{(\prime)} \ell \nu_\ell), \quad (28)$$

where $\tau(H)$ is the H -meson lifetime, and the maximum of the squared momentum transfer $q_{\max}^2 = (m_H - m_{\eta^{(\prime)}})^2$.

III. NUMERICAL ANALYSIS

A. Input parameters

We adopt the following parameters to do the numerical calculation. According to the Particle Data Group (PDG) [23], we take the charm-quark mass $m_c(\bar{m}_c) = 1.27 \pm 0.02$, b -quark mass $m_b(\bar{m}_b) = 4.18_{-0.02}^{+0.03}$ GeV; the η , η' , D and B -meson masses are $m_\eta = 0.5478$ GeV, $m_{\eta'} = 0.9578$ GeV, $m_{D^+} = 1.870$ GeV and $m_{B^+} = 5.279$ GeV, respectively; the lifetimes of D^+ and B^+ mesons are $\tau(B^+) = 1.638 \pm 0.004$ ps and $\tau(D^+) = 1.033 \pm 0.005$ ps, respectively; the current-quark-masses for the light u and d -quarks are $m_u = 2.16_{-0.26}^{+0.49}$ MeV and $m_d = 4.67_{-0.17}^{+0.48}$ MeV at the scale $\mu = 2$ GeV. As for the decay constants f_B and f_D , we take $f_B = 0.215_{-0.007}^{+0.007}$ GeV [10] and $f_D = 0.142 \pm 0.006$ [83]. The renormalization scale is set as the typical momentum flow $\mu_B = \sqrt{m_B^2 - \bar{m}_b^2} \approx 3$ GeV for B -meson decay or $\mu_D \approx 1.4$ GeV for D -meson decay. We also need to know the values of the non-perturbative vacuum condensates up to dimension-six, which include the double-quark condensates $\langle q\bar{q} \rangle$ and $\langle g_s \bar{q}q \rangle^2$, the quark-gluon condensate $\langle g_s \bar{q}\sigma T G q \rangle$, the four-quark condensate $\langle g_s^2 \bar{q}q \rangle^2$, the double-gluon condensate $\langle \alpha_s G^2 \rangle$ and the triple-gluon condensate $\langle g_s^3 f G^3 \rangle$, and etc. We take their values as [84–86],

$$\begin{aligned} \langle q\bar{q} \rangle &= (-2.417_{-0.114}^{+0.227}) \times 10^{-2} \text{ GeV}^3, \\ \langle g_s \bar{q}q \rangle^2 &= (2.082_{-0.697}^{+0.734}) \times 10^{-3} \text{ GeV}^6, \\ \langle g_s \bar{q}\sigma T G q \rangle &= (-1.934_{-0.103}^{+0.188}) \times 10^{-2} \text{ GeV}^5, \end{aligned}$$

$$\begin{aligned} \langle g_s^2 \bar{q}q \rangle^2 &= (7.420_{-2.483}^{+2.614}) \times 10^{-3} \text{ GeV}^6, \\ \langle \alpha_s G^2 \rangle &= 0.038 \pm 0.011 \text{ GeV}^4, \\ \langle g_s^3 f G^3 \rangle &\approx 0.045 \text{ GeV}^6. \end{aligned} \quad (29)$$

The ratio $\kappa = \langle s\bar{s} \rangle / \langle q\bar{q} \rangle = 0.74 \pm 0.03$ is given in Ref. [85]. In order to make the calculation more accurate, every vacuum condensates and current quark masses need to be run from their initial values at the scale μ_0 to the required scale by using the renormalization group equations (RGE) [54].

B. The η_q decay constant and the moments $\langle \xi_{2;\eta_q}^n \rangle$

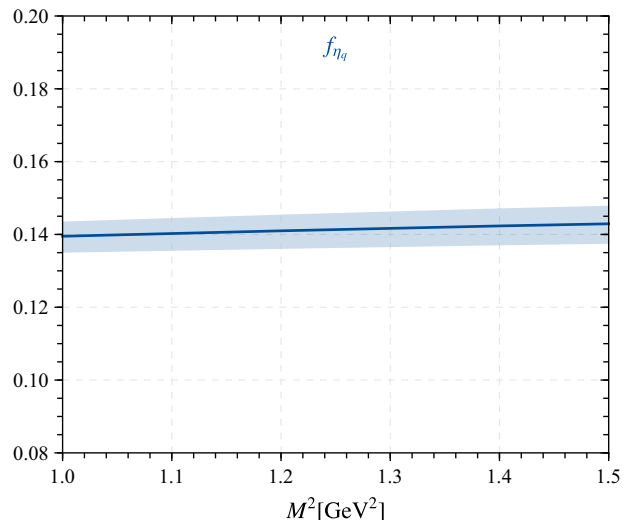


FIG. 1: (Color online) The η_q decay constant f_{η_q} versus the Borel parameter M^2 , where the shaded band indicates the uncertainties from the input parameters.

The continuum threshold parameter (s_0) and the Borel parameter M^2 are two important parameters for the sum rules analysis. When calculating the decay constant f_{η_q} , one may set its continuum threshold to be close to the squared mass of the η' meson, i.e. $s_0 = 0.95 \pm 0.1 \text{ GeV}^2$ [56]. To determine the allowable M^2 range, e.g. the Borel window, for the η_q decay constant, we adopt the following criteria,

- The continuum contribution is less than 30%;
- The contributions of the six-dimensional condensates are no more than 5%;
- The value of f_{η_q} is stable in the Borel window;
- The $\langle \xi_{2;\eta_q}^0 \rangle|_{\mu_0}$ is normalized in the Borel window, e.g. $\langle \xi_{2;\eta_q}^0 \rangle|_{\mu_0} = 1$.

We put the curves for the decay constant f_{η_q} versus the Borel parameter M^2 in Fig. 1, where the shaded

TABLE I: The decay constant f_{η_q} using the BFTSR approach. As a comparison, typical results derived from QCDSR and LQCD approaches have also been presented.

References	f_{η_q} [GeV]
This work (BFTSR)	$0.141^{+0.005}_{-0.005}$
QCDSR 2000 [56]	$0.144^{+0.004}_{-0.004}$
QCDSR 1998 [57]	0.168
LQCD 2021 [65]	$0.149^{+0.034}_{-0.023}$

band indicates the uncertainties from the errors of all the mentioned input parameters. The decay constant is flat in the allowable Borel window, which confirms the third criterion. Using the above four criteria and the chosen continuum threshold parameter, we put the numerical results of f_{η_q} in Table I. As a comparison, we also present several predictions using the QCDSR and LQCD approaches. Our predictions are in good agreement with the QCDSR 2000 [56] and the LQCD 2021 predictions within errors [65]. The reason why we are slightly different from QCDSR 2000 is that their calculation only includes the contributions up to five dimensional operators, and our present one includes the dimension-6 vacuum condensation terms. Using the determined f_{η_q} , we then determine the moments of its twist-2 LCDA. Similarly, several important conditions need to be satisfied before the moments of η_q LCDA can be determined [51].

Furthermore, in order to search for a suitable Borel window for the moments, one can take the similar criteria adopted for the traditional sum rules, i.e. keeping the dimension-six condensate's contribution to be no more than 5% and the continuum contribution to be no more than 40%. To determine the first two LCDA moments $\langle \xi_{2;\eta_q}^n \rangle|_{\mu_0}$ with $n = (2, 4)$, we set the continuum contributions to be less than 35% and 40%, respectively. We find that the allowable Borel windows for the two moments $\langle \xi_{2;\eta_q}^{2,4} \rangle|_{\mu}$ are $M^2 \in [1.782, 2.232]$ and $M^2 \in [2.740, 3.258]$, respectively. Numerical results of the first two moments $\langle \xi_{2;\eta_q}^{2,4} \rangle|_{\mu}$ can be obtained, which at the initial scale μ_0 are

$$\langle \xi_{2;\eta_q}^2 \rangle|_{\mu_0} = 0.253 \pm 0.014, \quad (30)$$

$$\langle \xi_{2;\eta_q}^4 \rangle|_{\mu_0} = 0.127 \pm 0.010. \quad (31)$$

C. The LCHO model parameters for $\phi_{2;\eta_q}$

TABLE II: The parameters $A_{2;\eta_q}$, $\beta_{2;\eta_q}$, B_2 , B_4 and the quark transverse momentum $\langle \mathbf{k}_{\perp}^2 \rangle_{\eta_q}$ by taking the constituent quark mass m_q to be (250, 300, 350) MeV, respectively.

m_q (MeV)	$A_{2;\eta_q}$ (GeV ⁻¹)	$\beta_{2;\eta_q}$ (GeV)	B_2	B_4	$\langle \mathbf{k}_{\perp}^2 \rangle_{\eta_q}$
250	39.909	0.589	0.100	0.073	0.121
300	40.606	0.564	0.155	0.108	0.123
350	42.921	0.549	0.219	0.149	0.126

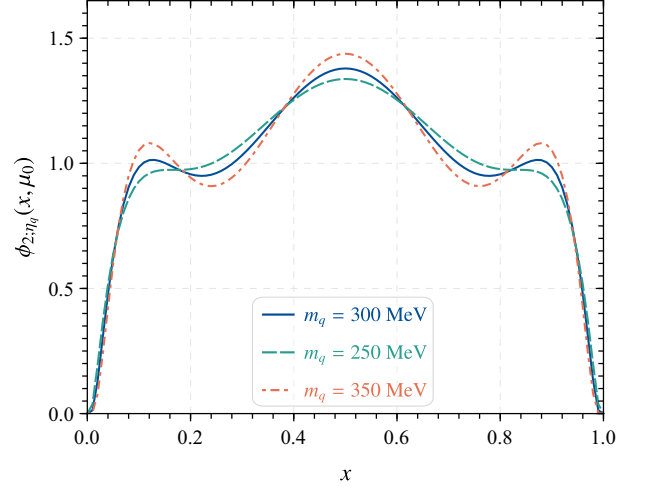


FIG. 2: (Color online) The LCHO model for the η_q twist-2 LCDA $\phi_{2;\eta_q}$ at the scale $\mu_0 = 1\text{ GeV}$ with the constituent quark mass $m_q = (250, 300, 350)$ MeV, respectively.

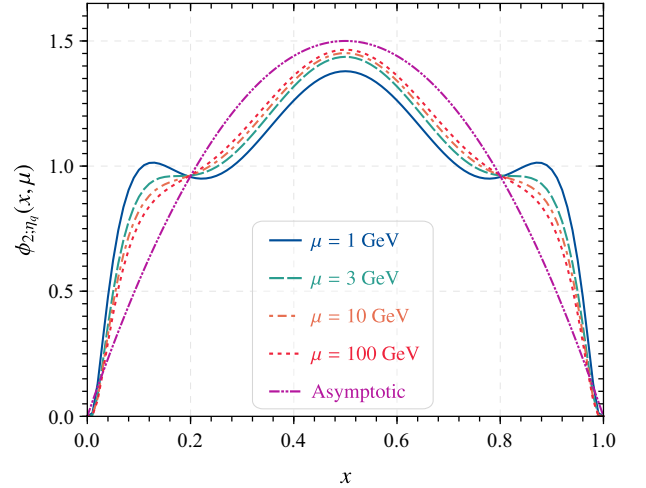


FIG. 3: (Color online) The LCHO model for the η_q twist-2 LCDA $\phi_{2;\eta_q}(x, \mu)$ at several typical scales with $m_q = 300$ MeV.

Combining the normalization condition (14), the probability formula for $q\bar{q}$ Fock state $P_{\eta_q} \approx 0.3$, and the moments $\langle \xi_{2;\eta_q}^{(2,4)} \rangle|_{\mu_0}$ shown in Eqs.(30, 31), the determined LCHO parameters are shown in Table II and their corresponding LCDA $\phi_{2;\eta_q}$ is given in Fig. 2. Its behavior of one peak with two humps is caused by $a_{2;\eta_q}^2(\mu_0) = 0.156 \pm 0.042$ and $a_{2;\eta_q}^4(\mu_0) = 0.055 \pm 0.005$, which is given by using their relations (18) to the moments $\langle \xi_{2;\eta_q}^n \rangle$ that can be calculated by using the sum rules (9). In this paper, we take $m_q = 300$ MeV to do the following calculation and use $\Delta m_q = \pm 50$ MeV to estimate

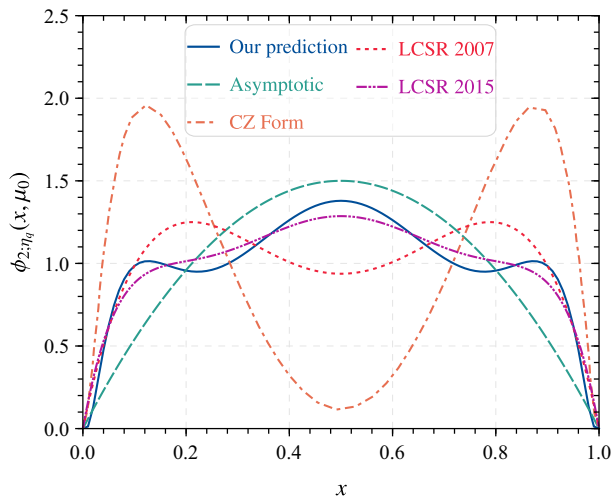


FIG. 4: (Color online) The η_q meson twist-2 LCDA $\phi_{2;\eta_q}(x, \mu_0)$. As a comparison, the asymptotic and CZ forms [88, 89] and the one derived using the LCSR approach [9, 10] are also presented.

its uncertainty. Table II shows that the parameters B_2 and B_4 and the quark transverse momentum $\langle \mathbf{k}_\perp^2 \rangle_{\eta_q}$ increase with the increment of constituent quark mass, but the harmonious parameter $\beta_{2;\eta_q}$ decreases gradually. Experimentally the average quark transverse momentum of pion, $\langle \mathbf{k}_\perp^2 \rangle_\pi$, is of the order $(300 \text{ MeV})^2$ approximately [87]. So it is reasonable to require $\sqrt{\langle \mathbf{k}_\perp^2 \rangle_{\eta_q}}$ have the value of about a few hundreds MeV [74]. For the case of $m_q = 300 \pm 50 \text{ MeV}$, we numerically obtain $\langle \mathbf{k}_\perp^2 \rangle_{\eta_q} = 0.123^{+0.003}_{-0.002} \approx (351^{+4}_{-3} \text{ MeV})^2$, which is reasonable and in some sense indicates the inner consistency of all the LCHO model parameters. Moreover, by using the RGE, one can get the $\phi_{2;\eta_q}(x, \mu)$ at any scale μ [54]. Fig. 3 shows the LCDA $\phi_{2;\eta_q}$ at several typical scales with $m_q = 300 \text{ MeV}$. At low scale, it shows double humped behavior and when the scale μ increases, the shape of $\phi_{2;\eta_q}$ becomes narrower; and when $\mu \rightarrow \infty$, it will tends to single-peak asymptotic behavior for the light mesons [] $\phi_{\eta_q}^{\text{as}}(x, \mu)|_{\mu \rightarrow \infty} = 6x(1-x)$.

We make a comparison of the properties of the LCHO model of the twist-2 LCDA $\phi_{2;\eta_q}$ with other theoretical predictions in Fig. 4. Fig. 4 gives the results for $\mu = \mu_0 = 1 \text{ GeV}$, where the asymptotic form [88], the CZ form [89] and the behaviors given by the LCSR 2007 [9] and LCSR 2015 [10] are presented. For the LCSR 2007 result, its double peaked behavior is caused by the keeping its Gegenbauer expansion only with the first term together with the approximation $a_{2;\eta_q}^2(\mu_0) = a_{2;\eta'_q}^2(\mu_0) = 0.25$ [9]. For the LCDA used in LCSR 2015 [10], its behavior is close to our present one. It is obtained by using the approximation that the twist-2 LCDA $\phi_{2;\eta_q}$ has the same behavior as that of the pion

twist-2 LCDA $\phi_{2;\pi}$, e.g. $a_{2;\eta_q}^2(\mu_0) = a_{2;\pi}^2(\mu_0) = 0.17$ and $a_{2;\eta'_q}^2(\mu_0) = a_{2;\pi}^2(\mu_0) = 0.06$, which are consistent with our Gegenbauer moments within errors ².

D. The TFFs and observable for the semileptonic decay $B(D)^+ \rightarrow \eta^{(\prime)} \ell^+ \nu_\ell$

One of the most important applications of the η_q -meson LCDAs is the semileptonic decay $H^+ \rightarrow \eta^{(\prime)} \ell^+ \nu_\ell$, whose main contribution in the QF scheme comes from the $|\eta_q\rangle$ -component. Here H^+ stands for B^+ or D^+ , respectively. And to derive the required $H^+ \rightarrow \eta^{(\prime)}$ TFFs, we take the mixing angle $\phi = (41.2^{+0.05}_{-0.06})^\circ$ [51].

The continuum threshold $s_0^{H \rightarrow \eta^{(\prime)}}$ and Borel parameters M^2 are two important parameters for the LCSR of the TFFs. As usual choice of treating the heavy-to-light TFFs, we set the continuum threshold as the one near the squared mass of the first excited state of D or B -meson, accordingly. And to fix the Borel window for the TFFs, we require the contribution of the continuum states to be less than 30%. The determined values agree with Refs.[10, 90], and we will take the following values to do our discussion

$$\begin{aligned} s_0^{D \rightarrow \eta} &= 7.0 \pm 0.5 \text{ GeV}^2, & M_{D \rightarrow \eta}^2 &= 3.0 \pm 0.5 \text{ GeV}^2. \\ s_0^{D \rightarrow \eta'} &= 7.0 \pm 0.5 \text{ GeV}^2, & M_{D \rightarrow \eta'}^2 &= 3.0 \pm 0.5 \text{ GeV}^2. \\ s_0^{B \rightarrow \eta} &= 37.0 \pm 1.0 \text{ GeV}^2, & M_{B \rightarrow \eta}^2 &= 18.0 \pm 2.0 \text{ GeV}^2. \\ s_0^{B \rightarrow \eta'} &= 37.0 \pm 1.0 \text{ GeV}^2, & M_{B \rightarrow \eta'}^2 &= 18.0 \pm 2.0 \text{ GeV}^2. \end{aligned}$$

TABLE III: Typical theoretical predictions on the TFFs $f_+^{H \rightarrow \eta^{(\prime)}}(0)$ at the large recoil point $q^2 = 0$.

	$f_+^{B \rightarrow \eta}(0)$	$f_+^{B \rightarrow \eta'}(0)$
This work (LCSR)	$0.145^{+0.009}_{-0.010}$	$0.128^{+0.008}_{-0.009}$
LCSR 2007 [9]	0.229 ± 0.035	0.188 ± 0.028
LCSR 2015 [10]	$0.168^{+0.041}_{-0.047}$	$0.130^{+0.036}_{-0.032}$
pQCD [92]	0.147	0.121
CLF [93]	0.220 ± 0.018	0.180 ± 0.016
LCSR 2013 [91]	0.238 ± 0.046	0.198 ± 0.039
	$f_+^{D \rightarrow \eta}(0)$	$f_+^{D \rightarrow \eta'}(0)$
This work (LCSR)	$0.329^{+0.021}_{-0.015}$	$0.294^{+0.021}_{-0.015}$
LCSR 2015 [10]	$0.429^{+0.165}_{-0.141}$	$0.292^{+0.113}_{-0.104}$
BES-III 2020 [27]	$0.39 \pm 0.04 \pm 0.01$	-
LFQM [94]	0.39	0.32
CCQM [95]	0.36(5)	0.36(5)
LCSR 2013 [91]	0.552(51)	0.458(105)

² Since the twist-2 parts dominant the TFFs, this consistency also explains why our following LCSR predictions for the TFFs are close in shape with those of Ref.[10].

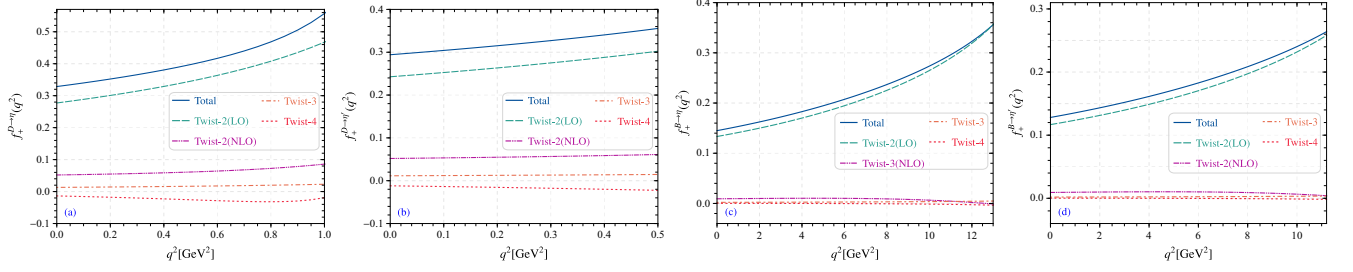


FIG. 5: (Color online) LCSR predictions on the TFFs $f_+^{H \rightarrow \eta^{(\prime)}}(q^2)$ with $H = B^+$ or D^+ in the allowable q^2 range, where the contributions from the twist-2, 3, 4 LCDAs are given separately. The twist-2 terms are given up to NLO QCD corrections.

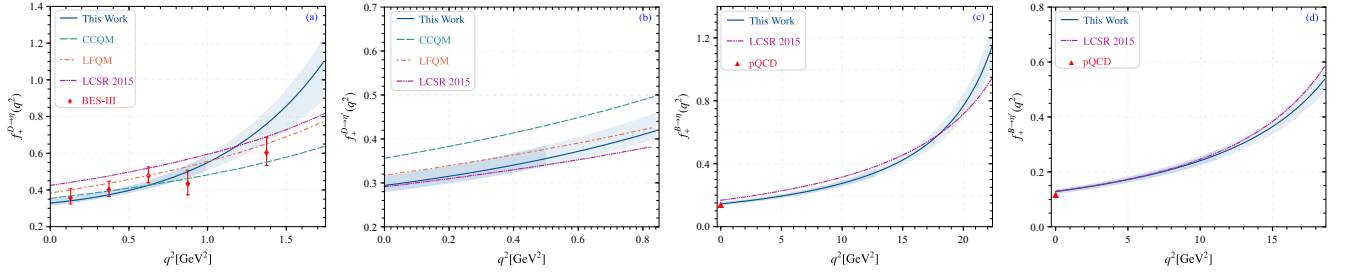


FIG. 6: (Color online) The TFFs $f_+^{H \rightarrow \eta^{(\prime)}}(q^2)$ in whole q^2 -region, where the solid line is the central value and the shaded band shows its uncertainty. The darker part of the shaded band is the LCSR prediction, and the remaining part is the extrapolated result. As a comparison, predictions using different theoretical approaches and the experimental data, such as CCQM [95], LFQM [94], LCSR [10], pQCD [92] and BESIII collaboration [27], are also presented.

Using Eqs.(2, 3) together with the LCSR (27) for the TFF $f_+^{H \rightarrow \eta_q}(q^2)$, we then get the results for $f_+^{H \rightarrow \eta^{(\prime)}}(q^2)$, where H represents B or D , respectively. Fig. 5 shows how the total TFFs $f_+^{H \rightarrow \eta^{(\prime)}}(q^2)$ change with the increment of q^2 , in which the twist-2 up to NLO QCD corrections, the twist-3 and the twist-4 contributions have been presented separately. Fig. 5 shows that the twist-2 terms dominant the TFFs. We also find that the NLO QCD corrections to the twist-2 terms are sizable and should be taken into consideration for a sound prediction. For examples, at the large recoil point, the twist-2 NLO terms give about 15.8% (17.6%) and 6.4% (7.2%) contributions to the total TFFs $f_+^{D \rightarrow \eta^{(\prime)}}(0)$ and $f_+^{B \rightarrow \eta^{(\prime)}}(0)$, respectively. Table III gives our present LCSR predictions for the TFFs $f_+^{D \rightarrow \eta^{(\prime)}}(0)$ and $f_+^{B \rightarrow \eta^{(\prime)}}(0)$. As a comparison, we have also presented the results derived from various theoretical approaches and experimental data in Table III, including the LCSR approach [9, 10, 91], the pQCD approach [92], the covariant light front (CLF) approach [93], the light front quark model (LFQM) approach [94], the covariant confining quark mode (CCQM) approach [95], and the BES-III Collaboration [27]. The uncertainties of the TFFs $f_+^{H \rightarrow \eta^{(\prime)}}(0)$ caused by different input parameters are listed as follows,

$$f_+^{B \rightarrow \eta}(0) = 0.145_{(-0.004)}^{(+0.004)} s_0 (-0.002)_{(-0.002)} M^2 (+0.007)_{(-0.007)} m_b f_B$$

$$\begin{aligned} & (+0.005)_{(-0.005)} f_{\eta_q} (+0.0001)_{(-0.0001)} \phi \\ & = 0.145_{-0.010}^{+0.009}, \end{aligned} \quad (32)$$

$$\begin{aligned} f_+^{B \rightarrow \eta'}(0) & = 0.128_{(-0.003)}^{(+0.003)} s_0 (+0.002)_{(-0.002)} M^2 (+0.006)_{(-0.006)} m_b f_B \\ & \quad (+0.005)_{(-0.005)} f_{\eta_q} (+0.0002)_{(-0.0001)} \phi \\ & = 0.128_{-0.009}^{+0.008}, \end{aligned} \quad (33)$$

$$\begin{aligned} f_+^{D \rightarrow \eta}(0) & = 0.329_{(-0.004)}^{(+0.003)} s_0 (+0.009)_{(-0.005)} M^2 (+0.016)_{(-0.009)} m_c f_D \\ & \quad (+0.010)_{(-0.010)} f_{\eta_q} (+0.0002)_{(-0.0003)} \phi \\ & = 0.329_{-0.015}^{+0.021}, \end{aligned} \quad (34)$$

$$\begin{aligned} f_+^{D \rightarrow \eta'}(0) & = 0.294_{(-0.004)}^{(+0.003)} s_0 (+0.009)_{(-0.005)} M^2 (+0.017)_{(-0.011)} m_c f_D \\ & \quad (+0.009)_{(-0.009)} f_{\eta_q} (+0.0002)_{(-0.0003)} \phi \\ & = 0.294_{-0.015}^{+0.021}. \end{aligned} \quad (35)$$

Here the second equations show the squared averages of all the mentioned errors.

The physically allowable ranges of the above four heavy-to-light TFFs are $m_\ell^2 \leq q^2 \leq (m_{D^+} - m_\eta)^2 \approx 1.75 \text{ GeV}^2$, $m_\ell^2 \leq q^2 \leq (m_{D^+} - m_{\eta'})^2 \approx 0.84 \text{ GeV}^2$, $m_\ell^2 \leq q^2 \leq (m_{B^+} - m_\eta)^2 \approx 22.40 \text{ GeV}^2$ and $m_\ell^2 \leq q^2 \leq (m_{B^+} - m_{\eta'})^2 \approx 18.67 \text{ GeV}^2$, respectively. The LCSR approach is applicable in low and intermediate q^2

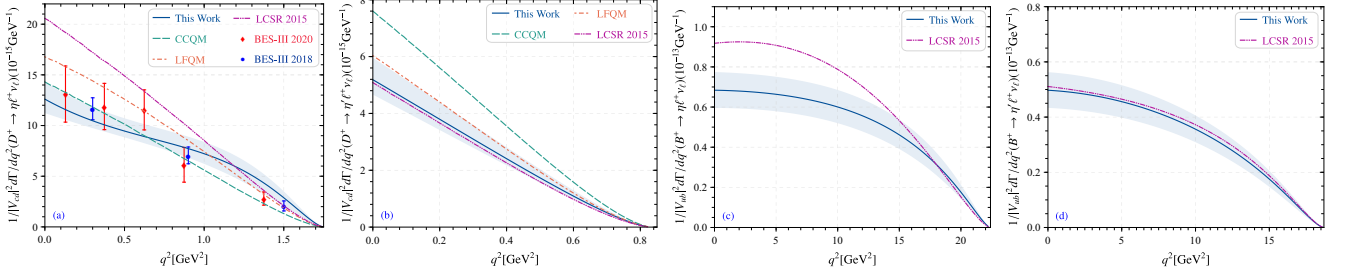


FIG. 7: (Color online) Differential decay widths for $B(D)^+ \rightarrow \eta^{(\prime)} \ell^+ \nu_\ell$ in whole q^2 -region, where the solid line is the central value and the shaded band shows its uncertainty. As a comparison, the predictions using different theoretical approaches and the experimental data, such as CCQM [95], LFQM [94], LCSR [10] and BESIII collaboration [26, 27], are also presented.

TABLE IV: Fitting parameters b_1 and b_2 for the TFFs $f_+^{H \rightarrow \eta^{(\prime)}}(q^2)$, where all input parameters are set to be their central values. Δ is the measure of the quality of extrapolation.

	$f_+^{D \rightarrow \eta}(q^2)$	$f_+^{D \rightarrow \eta'}(q^2)$	$f_+^{B \rightarrow \eta}(q^2)$	$f_+^{B \rightarrow \eta'}(q^2)$
b_1	-0.033	-0.680	-0.392	-0.397
b_2	37.901	23.961	-0.108	-0.308
Δ	0.761%	0.026%	0.341%	0.062%

region, which however can be extended to whole q^2 region via proper extrapolation approaches. In the present paper, we adopt the converging simplified series expansion (SSE) proposed in Refs.[96, 97] to do the extrapolation, which suggest a simple parameterization for the heavy-to-light TFF, e.g.

$$f_+^{H \rightarrow \eta^{(\prime)}}(q^2) = \frac{1}{1 - q^2/m_{R^*}^2} \sum_k b_k z^k(t, t_0) \quad (36)$$

where $m_{R^*} = m_{B^*} = 5.325 \text{ GeV}$ ($m_{D^*} = 2.010 \text{ GeV}$) [10] are vector meson resonances, $z(t, t_0)$ is a function

$$z(t, t_0) = \frac{\sqrt{t_+ - t} - \sqrt{t_+ - t_0}}{\sqrt{t_+ - t} + \sqrt{t_+ - t_0}}. \quad (37)$$

Here $t_\pm = (m_{H^+} \pm m_{\eta^{(\prime)}})^2$ and $t_0 = t_+(1 - \sqrt{1 - t_-/t_+})$ is a free parameter. The free parameter b_k can be fixed by requiring $\Delta < 1\%$, where the parameter Δ is used to measure the quality of extrapolation and it is defined as

$$\Delta = \frac{\sum_t |F_i(t) - F_i^{\text{fit}}(t)|}{\sum_t |F_i(t)|} \times 100, \quad (38)$$

where $t \in [0, \frac{1}{40}, \dots, \frac{40}{40}] \times 13.0(1.0) \text{ GeV}$ of η -meson, $t \in [0, \frac{1}{40}, \dots, \frac{40}{40}] \times 11.2(0.5) \text{ GeV}$ of η' -meson. The two coefficients $b_{1,2}$ with all input parameters are set as their central values are listed in Table IV. The qualities of extrapolation parameter Δ are less than $\sim 0.8\%$. The extrapolated TFFs in whole q^2 -region are given in Fig. 6, where some typical theoretical and experimental results

are presented as a comparison, such as CCQM [95], LFQM [94], LCSR 2015 [10], pQCD [92] and BESIII 2020 [27]. The solid lines in Fig. 6 denote the center values of the LCSR predictions, where the shaded areas are theoretical uncertainties from all the mentioned error sources. The thicker shaded bands represent the LCSR predictions, which have been extrapolated to physically allowable q^2 -region. Fig. 6 indicates that: 1) Our present LCSR prediction of $f_+^{D \rightarrow \eta}(q^2)$ is in good agreement with BESIII data [27]; 2) Our present LCSR prediction of $f_+^{D \rightarrow \eta'}(q^2)$ is consistent with the LFQM prediction [94] and the LCSR 2015 [10] predictions within errors; 3) Our present LCSR predictions of $f_+^{B \rightarrow \eta^{(\prime)}}(q^2)$ are close to the LCSR 2015 prediction [10], and their values at $q^2 = 0$ are consistent with the pQCD prediction [92] within errors.

Fig. 7 shows the differential decay widths for $B(D)^+ \rightarrow \eta^{(\prime)} \ell^+ \nu_\ell$ without CKM matrix elements. As a comparison, the predictions using different theoretical approaches and the experimental data, such as CCQM [95], LFQM [94], LCSR [10] and BESIII collaboration [26, 27], are also presented. The differential decay width $d\Gamma/|V_{cd}|dq^2(D^+ \rightarrow \eta \ell^+ \nu_\ell)$ agrees with the BESIII 2018 [26] and BESIII 2020 [27] within errors.

By matching the branching fractions and the decay lifetimes given by the PDG with the decay widths predicted by Eq.(28), one may derive the CKM matrix elements $|V_{ub}|$ and $|V_{cd}|$. We put our results in Table V, where the errors are caused by all the mentioned error sources and the PDG errors for the branching fractions and the decay lifetimes. Some typical measured values of $|V_{ub}|$ and $|V_{cd}|$ are also given in Table V. The predicted $|V_{cd}|$ is within the error range of experimental result BESIII 2020. Using the fixed CKM matrix elements, our final predictions of the branching function are: $\mathcal{B}(D \rightarrow \eta e \nu_e) = (1.11 \pm 0.07) \times 10^{-3}$, $\mathcal{B}(D \rightarrow \eta \mu \nu_\mu) = (1.04 \pm 0.11) \times 10^{-3}$, $\mathcal{B}(D \rightarrow \eta' e \nu_e) = (2.0 \pm 0.4) \times 10^{-4}$, $\mathcal{B}(B \rightarrow \eta \ell \nu_\ell) = (3.9 \pm 0.5) \times 10^{-5}$, $\mathcal{B}(B \rightarrow \eta' \ell \nu_\ell) = (2.3 \pm 0.8) \times 10^{-5}$, respectively.

TABLE V: CKM matrix elements $|V_{cd}|$ and $|V_{ub}|$ are obtained by different experimental groups according to different decay processes.

Mode	Channels	$ V_{cd} $
This work	$D^+ \rightarrow \eta e^+ \nu_e$	$0.236^{+0.017}_{-0.017}$
This work	$D^+ \rightarrow \eta \mu^+ \nu_\mu$	$0.228^{+0.017}_{-0.017}$
This work	$D^+ \rightarrow \eta' e^+ \nu_e$	$0.253^{+0.028}_{-0.032}$
BESIII 2020 [27]	$D^+ \rightarrow \eta \mu^+ \nu_\mu$	$0.242 \pm 0.028 \pm 0.033$
BESIII 2013 [15]	$D^+ \rightarrow \mu^+ \nu_\mu$	$0.221 \pm 0.006 \pm 0.005$
BaBar 2014 [16]	$D^0 \rightarrow \pi^- e^+ \nu_e$	$0.206 \pm 0.007 \pm 0.009$
CLEO 2009 [17]	$D \rightarrow \pi e^+ \nu_e$	$0.234 \pm 0.009 \pm 0.025$
HFLAV [18]	$D \rightarrow \pi \ell \nu_\ell$	$0.225 \pm 0.003 \pm 0.006$
LQCD 2019 [19]	$D \rightarrow \pi \ell \nu$	0.233 ± 0.137
PDG [23]	$D \rightarrow \pi \ell \nu$	$0.233 \pm 0.003 \pm 0.013$
	Channels	$ V_{ub} \times 10^{-3}$
This work	$B^+ \rightarrow \eta \ell^+ \nu_\ell$	$3.752^{+0.373}_{-0.351}$
This work	$B^+ \rightarrow \eta' \ell^+ \nu_\ell$	$3.888^{+0.688}_{-0.787}$
CLEO 2007 [14]	$B^0 \rightarrow \pi^- \ell^+ \nu$	$3.60 \pm 0.4 \pm 0.2$
HFLAV [18]	$B \rightarrow \pi \ell \nu_\ell$	$3.70 \pm 0.10 \pm 0.12$
BaBar 2011 [20]	$\bar{B} \rightarrow X_u \ell \bar{\nu}$	$4.33 \pm 0.24 \pm 0.15$
Belle [21]	$B \rightarrow X_u \ell \nu$	$4.09 \pm 0.39 \pm 0.18$
PDG [23]	$B \rightarrow \pi \ell \bar{\nu}$	3.82 ± 0.20
PDG [23]	$B \rightarrow X_u \ell \bar{\nu}$	$4.13 \pm 0.12 \pm 0.18$
LQCD 2015 [98]	$B \rightarrow \pi \ell \nu$	3.72 ± 0.16

IV. SUMMARY

In this paper, we have suggest a LCHO model (13) for the η_q -meson leading-twist LCDA $\phi_{2;\eta_q}(x, \mu)$, whose moments have been calculated by using the QCD sum rules based on the QCD background field. To compare with

the conventional Gegenbauer expansion for the LCDA, the LCHO model usually has better end-point behavior due to the BHL-prescription, which will be helpful to suppress the end-point singularity for the heavy-to-light meson decays. The QCD sum rules for the 0_{th}-order moment can be used to fix the η_q decay constant, and we obtain $f_{\eta_q} = 0.141 \pm 0.005$ GeV. As an explicit application of $\phi_{2;\eta_q}$, we then calculate the TFFs $B(D)^+ \rightarrow \eta^{(\prime)}$ under the QF scheme for the $\eta - \eta'$ mixing and by using the QCD light-cone sum rules up to twist-4 accuracy and by including the next-to-leading order QCD corrections to the dominant twist-2 part. Our LCSR prediction of TFFs are consistent with most of theoretical predictions and the recent BESIII data within errors. By applying those TFFs, we get the decay widths of $B(D)^+ \rightarrow \eta^{(\prime)} \ell^+ \nu_\ell$. The magnitudes of the CKM matrix elements $|V_{ub}|$ and $|V_{cd}|$ have also been discussed by inversely using the PDG values for the branching fractions and the decay lifetimes. The future more precise data at the high luminosity Belle II experiment [99] and super tau-charm factory [100] shall be helpful to test all those results.

V. ACKNOWLEDGMENTS

This work was supported in part by the Chongqing Graduate Research and Innovation Foundation under Grant No. CYB23011 and No.ydstd1912, by the National Natural Science Foundation of China under Grant No.12175025, No.12265010, No.12265009 and No.12147102, the Project of Guizhou Provincial Department of Science and Technology under Grant No.ZK[2021]024 and No.ZK[2023]142, and the Project of Guizhou Provincial Department of Education under Grant No.KY[2021]030, and the Key Laboratory for Particle Physics of Guizhou Minzu University No.GZMUZK[2022]PT01.

-
- [1] H. W. Ke, X. Q. Li and Z. T. Wei, “Determining the $\eta - \eta'$ mixing by the newly measured $BR(D(D_s) \rightarrow \eta(\eta') + \bar{l} + \nu_l)$ ”, Eur. Phys. J. C **69** (2010) 133.
 - [2] H. W. Ke, X. H. Yuan and X. Q. Li, “Fraction of the gluonium component in η' and η ”, Int. J. Mod. Phys. A **26** (2011) 4731.
 - [3] F. G. Cao, “Determination of the η - η' mixing angle”, Phys. Rev. D **85** (2012) 057501.
 - [4] F. J. Gilman and R. Kauffman, “The eta Eta-prime Mixing Angle”, Phys. Rev. D **36** (1987) 2761.
 - [5] P. Ball, J. M. Frere and M. Tytgat, “Phenomenological evidence for the gluon content of eta and eta-prime”, Phys. Lett. B **365** (1996) 367.
 - [6] T. Feldmann and P. Kroll, “Mixing of pseudoscalar mesons”, Phys. Scripta T **99** (2002) 13.
 - [7] P. Kroll and K. Passek-Kumericki, “The Two gluon components of the eta and eta-prime mesons to leading twist accuracy”, Phys. Rev. D **67** (2003) 054017.
 - [8] F. Ambrosino, A. Antonelli, M. Antonelli, F. Archilli, P. Beltrame, G. Bencivenni, S. Bertolucci, C. Bini, C. Bloise and S. Bocchetta, *et al.* “A Global fit to determine the pseudoscalar mixing angle and the gluonium content of the eta-prime meson”, JHEP **07** (2009) 105.
 - [9] P. Ball and G. W. Jones, “ $B \rightarrow \eta^{(\prime)}$ Form Factors in QCD”, JHEP **0708** (2007) 025.
 - [10] G. Duplancic and B. Melic, “Form factors of $B, B_s \rightarrow \eta'$ and $D, D_s \rightarrow \eta'$ transitions from QCD light-cone sum rules”, JHEP **1511** (2015) 138.
 - [11] T. Feldmann, “Quark structure of pseudoscalar mesons,” Int. J. Mod. Phys. A **15** (2000) 159.
 - [12] T. Feldmann, “Mixing and decay constants of pseudoscalar mesons: Octet singlet versus quark flavor basis”, Nucl. Phys. B Proc. Suppl. **74** (1999) 151.
 - [13] T. Feldmann, P. Kroll and B. Stech, “Mixing and decay constants of pseudoscalar mesons”, Phys. Rev. D **58** (1998) 114006.
 - [14] N. E. Adam *et al.* [CLEO Collaboration], “A Study of Exclusive Charmless Semileptonic B Decay and $|V_{ub}|$ ”,

- Phys. Rev. Lett. **99** (2007) 041802.
- [15] M. Ablikim *et al.* [BESIII Collaboration], “Precision measurements of $B(D^+ \rightarrow \mu^+\nu_\mu)$, the pseudoscalar decay constant f_{D^+} , and the quark mixing matrix element $|V_{cd}|$ ”, Phys. Rev. D **89** (2014) 051104.
- [16] J. P. Lees *et al.* [BaBar Collaboration], “Measurement of the $D^0 \rightarrow \pi^- e^+ \nu_e$ differential decay branching fraction as a function of q^2 and study of form factor parameterizations”, Phys. Rev. D **91** (2015) 052022.
- [17] D. Besson *et al.* [CLEO Collaboration], “Improved measurements of D meson semileptonic decays to π and K mesons”, Phys. Rev. D **80** (2009) 032005.
- [18] Y. S. Amhis *et al.* [HFLAV], “Averages of b-hadron, c-hadron, and τ -lepton properties as of 2018”, Eur. Phys. J. C **81** (2021) 226.
- [19] V. Lubicz *et al.* [ETM Collaboration], “Scalar and vector form factors of $D \rightarrow \pi(K)\ell\nu$ decays with $N_f = 2 + 1 + 1$ twisted fermions”, Phys. Rev. D **96** (2017) 054514.
- [20] J. P. Lees *et al.* [BaBar Collaboration], “Study of $\bar{B} \rightarrow X_u \ell \bar{\nu}$ decays in $B\bar{B}$ events tagged by a fully reconstructed B-meson decay and determination of $|V_{ub}|$ ”, Phys. Rev. D **86** (2012) 032004.
- [21] I. Bizjak *et al.* [Belle Collaboration], “Determination of $|V_{ub}|$ from measurements of the inclusive charmless semileptonic partial rates of B mesons using full reconstruction tags”, Phys. Rev. Lett. **95** (2005) 241801.
- [22] S. González-Solís and P. Masjuan, “Study of $B \rightarrow \pi \ell \nu_\ell$ and $B^+ \rightarrow \eta^{(\prime)} \ell^+ \nu_\ell$ decays and determination of $|V_{ub}|$ ”, Phys. Rev. D **98** (2018) 034027.
- [23] P. A. Zyla *et al.* [Particle Data Group], “Review of Particle Physics”, PTEP **2022** (2022) 083C01.
- [24] R. E. Mitchell *et al.* [CLEO Collaboration], “Observation of $D^+ \rightarrow \eta e^+ \nu(e)$ ”, Phys. Rev. Lett. **102** (2009), 081801.
- [25] J. Yelton *et al.* [CLEO Collaboration], “Studies of $D^+ \rightarrow \eta', \eta, \phi e^+ \nu_e$ ”, Phys. Rev. D **84** (2011), 032001.
- [26] M. Ablikim *et al.* [BESIII Collaboration], “Study of the decays $D^+ \rightarrow \eta^{(\prime)} e^+ \nu_e$ ”, Phys. Rev. D **97** (2018) 092009.
- [27] M. Ablikim [BESIII Collaboration], “First Observation of $D^+ \rightarrow \eta \mu^+ \nu_\mu$ and Measurement of Its Decay Dynamics”, Phys. Rev. Lett. **124** (2020) 231801.
- [28] B. Aubert *et al.* [BaBar Collaboration], “Measurements of $B \rightarrow \{\pi, \eta, \eta'\} \ell \nu_\ell$ Branching Fractions and Determination of $|V_{ub}|$ with Semileptonically Tagged B Mesons”, Phys. Rev. Lett. **101** (2008) 081801.
- [29] P. del Amo Sanchez *et al.* [BaBar Collaboration], “Measurement of the $B^0 \rightarrow \pi^\ell \ell^+ \nu$ and $B^+ \rightarrow \eta^{(\prime)} \ell^+ \nu$ Branching Fractions, the $B^0 \rightarrow \pi^- \ell^+ \nu$ and $B^+ \rightarrow \eta \ell^+ \nu$ Form-Factor Shapes, and Determination of $|V_{ub}|$ ”, Phys. Rev. D **83** (2011) 052011.
- [30] C. Beleño *et al.* [Belle Collaboration], “Measurement of the decays $B \rightarrow \eta \ell \nu_\ell$ and $B \rightarrow \eta' \ell \nu_\ell$ in fully reconstructed events at Belle”, Phys. Rev. D **96** (2017) 091102.
- [31] U. Gebauer *et al.* [Belle Collaboration], “Measurement of the branching fractions of the $B^+ \rightarrow \eta \ell^+ \nu_\ell$ and $B^+ \rightarrow \eta' \ell^+ \nu_\ell$ decays with signal-side only reconstruction in the full q^2 range”, Phys. Rev. D **106** (2022) 032013.
- [32] H. Y. Cheng and K. C. Yang, “Charmless Hadronic B Decays into a Tensor Meson”, Phys. Rev. D **83** (2011) 034001 (2011).
- [33] V. M. Braun and I. E. Filyanov, “QCD Sum Rules in Exclusive Kinematics and Pion Wave Function”, Z. Phys. C **44** (1989) 157.
- [34] I. I. Balitsky, V. M. Braun and A. V. Kolesnichenko, “Radiative Decay $\Sigma^+ \rightarrow p\gamma$ in Quantum Chromodynamics”, Nucl. Phys. B **312** (1989) 509.
- [35] V. L. Chernyak and I. R. Zhitnitsky, “B meson exclusive decays into baryons”, Nucl. Phys. B **345** (1990) 137.
- [36] P. Ball, V. M. Braun and H. G. Dosch, “Form-factors of semileptonic D decays from QCD sum rules”, Phys. Rev. D **44** (1991) 3567.
- [37] S. J. Brodsky, T. Huang and G. P. Lepage, “Hadronic wave functions and high momentum transfer interactions in quantum chromodynamics”, Conf. Proc. C **810816** (1981) 143. SLAC-PUB-16520.
- [38] G. P. Lepage, S. J. Brodsky, T. Huang and P. B. Mackenzie, “Hadronic Wave Functions in QCD”, CLNS-82-522.
- [39] T. Huang, X. N. Wang, X. D. Xiang and S. J. Brodsky, “The Quark Mass and Spin Effects in the Mesonic Structure”, Phys. Rev. D **35** (1987) 1013.
- [40] T. Huang and Z. Huang, “Quantum Chromodynamics in Background Fields”, Phys. Rev. D **39** (1989) 1213.
- [41] M. A. Shifman, A. I. Vainshtein and V. I. Zakharov, “QCD and Resonance Physics. Theoretical Foundations”, Nucl. Phys. B **147** (1979) 385.
- [42] W. Hubschmid and S. Mallik, “Operator Expansion At Short Distance In QCD”, Nucl. Phys. B **207** (1982) 29.
- [43] J. Govaerts, F. de Viron, D. Gusbin and J. Weyers, “QCD Sum Rules and Hybrid Mesons”, Nucl. Phys. B **248** (1984) 1.
- [44] L. J. Reinders, H. Rubinstein and S. Yazaki, “Hadron Properties from QCD Sum Rules”, Phys. Rept. **127** (1985) 1.
- [45] V. Elias, T. G. Steele and M. D. Scadron, “ $q\bar{q}$ and Higher Dimensional Condensate Contributions to the Nonperturbative Quark Mass”, Phys. Rev. D **38** (1988) 1584.
- [46] Y. Zhang, T. Zhong, H. B. Fu, W. Cheng and X. G. Wu, “Ds-meson leading-twist distribution amplitude within the QCD sum rules and its application to the $B_s \rightarrow D_s$ transition form factor”, Phys. Rev. D **103** (2021) 114024.
- [47] T. Zhong, Y. Zhang, X. G. Wu, H. B. Fu and T. Huang, “The ratio $\mathcal{R}(D)$ and the D -meson distribution amplitude”, Eur. Phys. J. C **78** (2018) 937.
- [48] H. B. Fu, L. Zeng, W. Cheng, X. G. Wu and T. Zhong, “Longitudinal leading-twist distribution amplitude of the J/ψ meson within the background field theory”, Phys. Rev. D **97** (2018) 074025.
- [49] Y. Zhang, T. Zhong, X. G. Wu, K. Li, H. B. Fu and T. Huang, “Uncertainties of the $B \rightarrow D$ transition form factor from the D-meson leading-twist distribution amplitude”, Eur. Phys. J. C **78** (2018) 76.
- [50] H. B. Fu, X. G. Wu, W. Cheng and T. Zhong, “ ρ -meson longitudinal leading-twist distribution amplitude within QCD background field theory”, Phys. Rev. D **94** (2016) 074004.
- [51] D. D. Hu, H. B. Fu, T. Zhong, L. Zeng, W. Cheng and X. G. Wu, “ η -meson leading-twist distribution amplitude within QCD sum rule approach and its application to the semi-leptonic decay $D_s^+ \rightarrow \eta \ell^+ \nu_\ell$ ”, Eur. Phys. J. C **82** (2022) 12.
- [52] G. S. Bali, S. Collins, S. Dürr and I. Kanamori,

- “ $D_s \rightarrow \eta, \eta'$ semileptonic decay form factors with disconnected quark loop contributions”, *Phys. Rev. D* **91** (2015) 014503.
- [53] S. Cheng, A. Khodjamirian and A. V. Rusov, “Pion light-cone distribution amplitude from the pion electromagnetic form factor”, *Phys. Rev. D* **102** (2020) 074022.
- [54] T. Zhong, Z. H. Zhu, H. B. Fu, X. G. Wu and T. Huang, “Improved light-cone harmonic oscillator model for the pionic leading-twist distribution amplitude”, *Phys. Rev. D* **104** (2021) 016021.
- [55] P. Ball and R. Zwicky, “New results on $B \rightarrow \pi, K, \eta$ decay formfactors from light-cone sum rules”, *Phys. Rev. D* **71** (2005) 014015.
- [56] F. De Fazio and M. R. Pennington, “Radiative ϕ meson decays and $\eta - \eta'$ mixing: A QCD sum rule analysis”, *JHEP* **07** (2000) 051.
- [57] A. Ali, G. Kramer and C. D. Lu, “Experimental tests of factorization in charmless nonleptonic two-body B decays”, *Phys. Rev. D* **58** (1998) 094009.
- [58] N. Dhiman, H. Dahiya, C. R. Ji and H. M. Choi, “Study of twist-2 distribution amplitudes and the decay constants of pseudoscalar and vector heavy mesons in light-front quark model”, *PoS LC2019* (2019) 038.
- [59] C. W. Hwang, “Analyses of decay constants and light-cone distribution amplitudes for S -wave heavy meson”, *Phys. Rev. D* **81** (2010) 114024.
- [60] C. Q. Geng, C. C. Lih and C. Xia, “Some heavy vector and tensor meson decay constants in light-front quark model”, *Eur. Phys. J. C* **76** (2016) 313.
- [61] H. M. Choi, “Decay constants and radiative decays of heavy mesons in light-front quark model”, *Phys. Rev. D* **75** (2007) 073016.
- [62] D. Dercks, H. Dreiner, M. E. Krauss, T. Opferkuch and A. Reinert, “R-Parity Violation at the LHC”, *Eur. Phys. J. C* **77** (2017) 856.
- [63] D. Becirevic, P. Boucaud, J. P. Leroy, V. Lubicz, G. Martinelli, F. Mescia and F. Rapuano, “Nonperturbatively improved heavy - light mesons: Masses and decay constants”, *Phys. Rev. D* **60** (1999) 074501.
- [64] A. Bazavov *et al.* [Fermilab Lattice and MILC], “Charmed and Light Pseudoscalar Meson Decay Constants from Four-Flavor Lattice QCD with Physical Light Quarks”, *Phys. Rev. D* **90** (2014) 074509.
- [65] G. S. Bali *et al.* [RQCD Collaboration], “asses and decay constants of the η and η' mesons from lattice QCD”, *JHEP* **08** (2021) 137.
- [66] G. Cvetič, C. S. Kim, G. L. Wang and W. Namgung, “Decay constants of heavy meson of 0-state in relativistic Salpeter method”, *Phys. Lett. B* **596** (2004) 84.
- [67] G. L. Wang, “Decay constants of heavy vector mesons in relativistic Bethe-Salpeter method”, *Phys. Lett. B* **633** (2006) 492.
- [68] S. Bhatnagar, S. Y. Li and J. Mahecha, “power counting of various Dirac covariants in hadronic Bethe-Salpeter wavefunctions for decay constant calculations of pseudoscalar mesons”, *Int. J. Mod. Phys. E* **20** (2011) 1437.
- [69] D. S. Hwang and G. H. Kim, “Decay constants of B, B^* and D, D^* mesons in relativistic mock meson model”, *Phys. Rev. D* **55** (1997) 6944.
- [70] S. Capstick and S. Godfrey, “Pseudoscalar Decay Constants in the Relativized Quark Model and Measuring the CKM Matrix Elements”, *Phys. Rev. D* **41** (1990) 2856.
- [71] D. Ebert, R. N. Faustov and V. O. Galkin, “Relativistic treatment of the decay constants of light and heavy mesons”, *Phys. Lett. B* **635** (2006) 93.
- [72] B. H. Yazarloo and H. Mehraban, “Study of B and B_s mesons with a Coulomb plus exponential type potential”, *EPL* **116** (2016) 31004.
- [73] X. H. Guo and T. Huang, “Hadronic wavefunctions in D and B decays”, *Phys. Rev. D* **43** (1991) 2931.
- [74] T. Huang, B. Q. Ma and Q. X. Shen, “Analysis of the pion wavefunction in light cone formalism”, *Phys. Rev. D* **49** (1994) 1490.
- [75] W. Jaus, “Relativistic constituent quark model of electroweak properties of light mesons”, *Phys. Rev. D* **44** (1991) 2851.
- [76] H. M. Choi and C. R. Ji, “Light cone quark model predictions for radiative meson decays”, *Nucl. Phys. A* **618** (1997) 291.
- [77] C. R. Ji, P. L. Chung and S. R. Cotanch, “Light cone quark model axial vector meson wave function”, *Phys. Rev. D* **45** (1992) 4214.
- [78] X. G. Wu and T. Huang, “Kaon Electromagnetic Form-Factor within the k(T) Factorization Formalism and It’s Light-Cone Wave Function”, *JHEP* **04** (2008) 043 (2008).
- [79] X. G. Wu and T. Huang, “Constraints on the Light Pseudoscalar Meson Distribution Amplitudes from Their Meson-Photon Transition Form Factors”, *Phys. Rev. D* **84** (2011) 074011 (2011).
- [80] T. Huang, T. Zhong and X. G. Wu, “Determination of the pion distribution amplitude”, *Phys. Rev. D* **88**, 034013 (2013).
- [81] X. G. Wu, T. Huang and T. Zhong, “Information on the Pion Distribution Amplitude from the Pion-Photon Transition Form Factor with the Belle and BaBar Data”, *Chin. Phys. C* **37**, 063105 (2013).
- [82] G. Duplancic, A. Khodjamirian, T. Mannel, B. Melic and N. Offen, “Light-cone sum rules for $B \rightarrow \pi$ form factors revisited”, *JHEP* **04** (2008) 014.
- [83] H. B. Fu, X. G. Wu, H. Y. Han, Y. Ma and T. Zhong, “ $|V_{cb}|$ from the semileptonic decay $B \rightarrow D\ell\bar{\nu}_\ell$ and the properties of the D meson distribution amplitude”, *Nucl. Phys. B* **884** (2014) 172.
- [84] P. Colangelo and A. Khodjamirian, “QCD sum rules, a modern perspective,” arXiv:hep-ph/0010175 [hep-ph].
- [85] S. Narison, “Mini-review on QCD spectral sum rules”, *Nucl. Part. Phys. Proc.* **258** (2015) 189.
- [86] S. Narison, “Improved $f_{D^{*(s)}}, f_{B^{*(s)}}$ and f_{B_c} from QCD Laplace sum rules,” *Int. J. Mod. Phys. A* **30** (2015) 1550116.
- [87] W. J. Metcalf, I. J. R. Aitchison, J. LeBritton, D. McCal, A. C. Melissinos, A. P. Contogouris, S. Papadopoulos, J. Alspector, S. Borenstein and G. R. Kalbfleisch, *et al.* “The Magnitude of Parton Intrinsic Transverse Momentum”, *Phys. Lett. B* **91** (1980) 275.
- [88] G. P. Lepage and S. J. Brodsky, “Exclusive Processes in Perturbative Quantum Chromodynamics,” *Phys. Rev. D* **22**, 2157 (1980).
- [89] V. L. Chernyak and A. R. Zhitnitsky, “Exclusive Decays of Heavy Mesons,” *Nucl. Phys. B* **201**, 492 (1982).
- [90] Z. G. Wang, “ $B - S$ transition formfactors with the light-cone QCD sum rules”, *Eur. Phys. J. C* **75** (2015) 50.
- [91] N. Offen, F. A. Porkert and A. Schäfer, “Light-

- cone sum rules for the $D_s \rightarrow \eta^{(\prime)} \ell \nu_\ell$ form factor”, *Phys. Rev. D* **88** (2013) 034023.
- [92] Y. Y. Charng, T. Kurimoto and H. n. Li, “Gluonic contribution to $B \rightarrow \eta^{(\prime)}$ form factors”, *Phys. Rev. D* **74** (2006) 074024.
- [93] C. H. Chen, Y. L. Shen and W. Wang, “ $|V(ub)|$ and $B \rightarrow \eta^{(\prime)}$ Form Factors in Covariant Light Front Approach”, *Phys. Lett. B* **686** (2010) 118.
- [94] R. C. Verma, “Decay constants and form factors of s-wave and p-wave mesons in the covariant light-front quark model”, *J. Phys. G* **39** (2012) 025005.
- [95] M. A. Ivanov, J. G. Körner, J. N. Pandya, P. Santorelli, N. R. Soni and C. T. Tran, “Exclusive semileptonic decays of D and D_s mesons in the covariant confining quark model”, *Front. Phys. (Beijing)* **14** (2019) 64401.
- [96] C. Bourrely, I. Caprini and L. Lellouch, “Model-independent description of $B \rightarrow \pi \ell \nu$ decays and a determination of $|V_{ub}|$ ”, *Phys. Rev. D* **79** (2009) 013008.
- [97] A. Bharucha, T. Feldmann and M. Wick, “Theoretical and Phenomenological Constraints on Form Factors for Radiative and Semi-Leptonic B -Meson Decays”, *JHEP* **09** (2010) 090.
- [98] J. A. Bailey *et al.* [Fermilab Lattice and MILC], “ $|V_{ub}|$ from $B \rightarrow \pi \ell \nu$ decays and (2+1)-flavor lattice QCD”, *Phys. Rev. D* **92** (2015) 014024.
- [99] E. Kou *et al.* [Belle-II], “The Belle II Physics Book,” *PTEP* **2019**, 123C01 (2019).
- [100] M. Achasov, X. C. Ai, R. Aliberti, Q. An, X. Z. Bai, Y. Bai, O. Bakina, A. Barnyakov, V. Blinov and V. Bobrovnikov, *et al.* “STCF Conceptual Design Report: Volume I - Physics & Detector,” arXiv:2303.15790 [hep-ex].